SGG✩SGS sc|nat

CrossMark

^{10}Be surface exposure dating of the last deglaciation in the Aare Valley, Switzerland

Lorenz Wüthrich[1,2] · Ezequiel Garcia Morabito[1,2] · Jana Zech[1] · Mareike Trauerstein[1] · Heinz Veit[1] · Christian Gnägi[1] · Silke Merchel[3] · Andreas Scharf[3] · Georg Rugel[3] · Marcus Christl[4] · Roland Zech[1,2]

Abstract

The combined Rhone and Aare Glaciers presumably reached their last glacial maximum (LGM) extent on the Swiss Plateau prior to 24 ka. Two well-preserved, less extensive moraine stades, the Gurten and Bern Stade, document the last deglaciation of the Aare Valley, yet age constraints are very scarce. In order to establish a more robust chronology for the glacial/deglacial history of the Aare Valley, we applied ^{10}Be surface exposure dating on eleven boulders from the Gurten and Bern Stade. Several exposure ages are of Holocene age and likely document post-depositional processes, including boulder toppling and quarrying. The remaining exposure ages, however yield oldest ages of 20.7 ± 2.2 ka for the Gurten Stade and 19.0 ± 2.0 ka for the Bern Stade. Our results are in good agreement with published chronologies from other sites in the Alps.

Keywords Pleistocene · Cosmogenic nuclides · Exposure dating · Alpine foreland

1 Introduction

Moraines document the variable extent of glaciers in the past and are key terrestrial archives to reconstruct and understand past climate changes and landscape history. During the last glaciation (Würm, Weichsel, or also referred to as Birrfeld Glacial in Switzerland), vast parts of Switzerland were covered with ice (Bini et al. 2009). Remnants of moraines and till indicate even more extensive earlier glaciations, referred to as Beringen and Möhlin Glacials, respectively (Graf 2009; Preusser et al. 2011; Keller and Krayss 2011). The Swiss Plateau is undoubtedly an important area to investigate (i) extent and timing of past glaciations, (ii) glacial erosion and particularly glacial

over-deepening (Schlüchter 1987; Preusser et al. 2010; Haeberli et al. 2016) and (iii) past climate changes.

During the last glacial, i.e. between marine isotope stage (MIS) 5d and MIS 2 (110–14 ka; Lisiecki and Raymo 2005), the Alpine glaciers advanced several times into the foreland, yet timing and extent are poorly constrained for most of these events (Preusser et al. 2011). Graf (2009) distinguished two glacial phases during MIS 2 on the Swiss Plateau and dubbed those Lindmühle and Birmenstorf Glaciations. The Lindmühle Glaciation probably occurred just after ∼ 29 ka (Preusser and Graf 2002), while the more extensive Birmenstorf Glaciation occurred a bit later but prior to ∼ 24 ka (Ivy-Ochs et al. 2004, 2006a; Reber et al. 2014). After the last glacial, the glaciers retreated from the foreland, interrupted by several re-advances of the decaying glaciers, which left well-preserved moraines (Keller and Krayss 2005a, b, 2011; Graf 2009; Reber et al. 2014). Wirsig et al. (2016) documented a rapid thinning of the glaciers in the high Alps with the onset of the Lateglacial at ∼ 18.5 ka. Several re-advances occurred during the Lateglacial, but they did not reach the forelands again and were restricted to the Alpine valleys. The oldest and most extensive Lateglacial advance, is dated to ∼ 17 ka (Ivy-Ochs et al. 2006b) and has been suggested to coincide with the Heinrich Event 1, a massive iceberg discharge and

---

Editorial handling: Chr. Schlüchter.

✉ Lorenz Wüthrich
loeru@live.com

1   Institute of Geography, University of Bern, Bern, Switzerland

2   Oeschger Center for Climate Change Research, University of Bern, Bern, Switzerland

3   Helmholtz-Zentrum, Dresden-Rossendorf, Dresden, Germany

4   Laboratory of Ion Beam Physics, ETH Zurich, Zurich, Switzerland

Ⓑ Birkhäuser

deposition of ice-rafted detritus in the North Atlantic (Heinrich 1988; Hemming 2004). For the present study, we applied ^{10}Be surface exposure dating on eleven boulders from the Gurten and Bern Stade in order to constrain the deglaciation history of the decaying Aare Glacier.

1.1 Regional and local context

The Aare Valley between Thun and Bern (Fig. 1) is in the transition zone between the high mountains of the Bernese Oberland and the Swiss Plateau. The landscape is characterized by rolling hills, which consist of Tertiary Molasse deposits and are mostly covered by Quaternary glacial- and glaciofluvial sediments. From old to young, the Seftigschwand, Gurten and Bern Stades have been mapped as the most prominent moraines in the Aare Valley (Fig. 1, Kellerhals et al. 2000).

During the LGM, the Aare Glacier merged with the much larger Rhone Glacier and covered the area in the vicinity of Bern with more than $\sim$ 300 m thick ice (Fig. 1, Bini et al. 2009). The source area of the glacier was located south-east of Bern on the northern side of the Alps (Reber and Schlunegger 2016). This is in contrast to the other Alpine LGM glaciers in Switzerland, which had their source area south of the Alpine weather divide (Florineth and Schlüchter 2000; Luetscher et al. 2015; Reber and
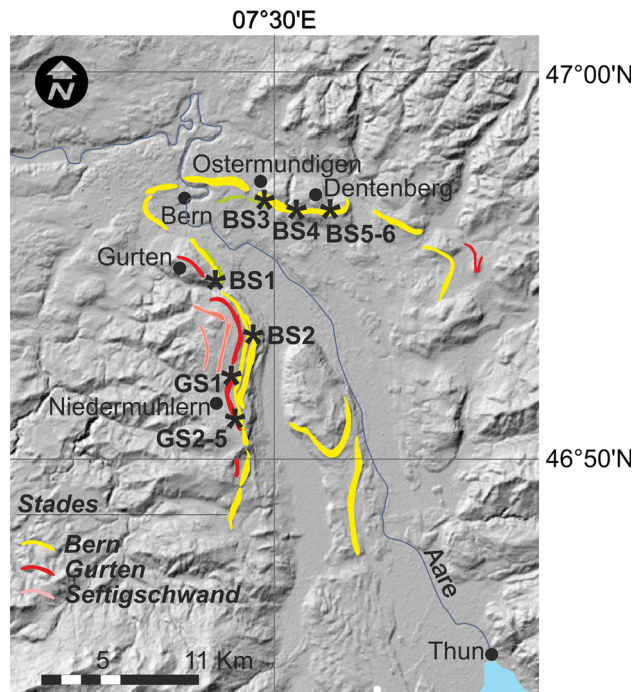

Fig. 1 Digital terrain model of the Aare Valley between Bern and Thun, with major stades of the former Aare Glacier after Kellerhals et al. (2000). Stars mark the sample locations on the Gurten Stade (GS1–5) and Bern Stade (BS1–6). Source of the Map: Federal Office of Topography

Schlunegger 2016; Becker et al. 2016). The stratigraphically oldest lateral moraines in the Aare Valley are mapped as Seftigschwand Stade and probably correlate with the maximum advance of the Rhone glacier (Kellerhals et al. 2000; Bini et al. 2009). The retreat from the LGM stade occured likely $\sim$ 24 ka ago (recalculated using the same scaling as for the boulders presented in this paper; see below) based on surface exposure ages from Steinhof of the Rhone Glacier (Ivy-Ochs et al. 2004, 2006a). As no boulders are available on the Seftigschwand moraine, the true age of the maximum advance of the LGM Aare glacier remains elusive.

The Gurten Stade documents a first still-stand or re-advance of the Aare Glacier after the LGM. At this time, the Aare and Rhone Glaciers were still merged, as no terminal moraines can be linked with Gurten Stade. However, its lateral moraines south of Bern are well preserved on top of the Gurten hill ($\sim$ 850 m) and along the Aare Valley, e.g. near Niedermuhlern ($\sim$ 900 m).

The Bern Stade has pronounced, well visible ridges and a terminal moraine in Bern ($\sim$ 560 m above sea level).

The Bern Stade marks a second pronounced still-stand or re-advance during deglaciation of the Aare Valley. It is characterized by well-preserved lateral moraines, as well as end moraines ($\sim$ 560 m above sea level), which are located in and around the city of Bern. Therefore, the Aare and Rhone Glaciers must have been separated by then. Its lateral moraines can be traced southward reaching altitudes of almost 700 m along the Gurten hill, as well as south-eastward reaching altitudes of $\sim$ 750 m along the Oster-mundigen- and Dentenberg (Fig. 1).

Just inside the Bern Stade, a few more glacial deposits have been mapped. These document minor still-stands or re-advances before the Aare Valley became ice-free (Kellerhals et al. 2000).

In summary, numerous studies have investigated the glacial deposits on the Swiss Plateau and in the Aare Valley (see also Schlüchter 1976, 1988; Preusser and Schlüchter 2004; Dehnert et al. 2010; Akçar et al. 2011), yet the extent and exact timing of their retreat of the Aare Glacier during the last glacial and the last deglaciation remain vague. We present our results in the context with other glacial chronologies from the Alps and discuss possible climate forcings.

2 Materials and methods

2.1 Sampling

The Samples from Gurten stade were taken from the well visible lateral moraine in Niedermulern (Figs. 1 and 2). We

Fig. 2 Pictures of the sampled boulders

sampled five boulders for surface exposure dating (GS1–5, Figs. 1 and 2). From the moraines of Bern Stade we sampled two boulders (BS 1 and BS 2) on the Gurten hill, one on Ostermundigenberg (BS 3) and three on Dentenberg (BS 4–6) (Figs. 1 and 2). Regarding the sampling strategy, we followed whenever possible the suggestions by Akçar et al. (2011). They imply that (1) the lithology of the boulder must be appropriate, (2) the boulder should lie on the moraine crest, (3) displacement and tilting should be avoided by using boulders as large as possible, (4) flat topped boulders should be favoured and (5) marks of weathering should be considered as problematic. All samples meet the criteria for (1) as they are all granitic boulders. Criteria (2) is fulfilled for all samples but BS 3, BS 4, GS 4 and GS 5 which were found on the slope of the respective moraines but still in a stable position i.e. their bases are embedded in the sediment. If possible, we considered boulders with a height > 1 m (criterium 3). BS 3, BS 4 and GS 4 have a height of < 1 m. All boulders but BS 1, GS 2, GS 4 and GS 5 are flat topped and fulfil criterium (4). The only boulder that shows signs of weathering (criteria 5) is BS 1, which is broken apart. On the other samples we did neither detect physical nor chemical weathering.

Approximately 500 g samples, 2–4 cm thick, were collected from the top of the boulders using hammer and chisel. Coordinates were recorded with a handheld GPS device and double-checked on the topographic and geologic maps. All boulders were documented photographically.

2.2 ^{10}Be surface exposure dating

In the last decades, ^{10}Be surface exposure dating has become an important tool for dating geomorphic features (Phillips et al. 2016). When applied to boulders on moraines, the exposure age ideally reflects the time since deposition and moraine stabilization. The principle of the method relies on the production and accumulation of in situ ^{10}Be when neutrons (Lal 1991) and muons (Heisinger et al. 2002a, b; Braucher et al. 2003) interact with the oxygen and silicon in quartz (Gosse and Phillips 2001). The production rate decreases with depth, so that erosion, shielding (rock, snow etc.), anthropogenic plucking, exhumation or toppling of the boulder can on the one hand all lead to an underestimation of the deposition age. On the other hand, inheritance could theoretically result in too old exposure ages due to pre-exposure of samples before deposition. At mid-latitudes, the probability for inheritance is generally assumed to be much lower than the probability that boulders were affected by post-depositional, common geomorphological processes (Heyman et al. 2011; Graf et al. 2015). This often justifies to interpret the oldest

boulder(s) as being closest to the deposition time of the moraine.

2.3 Laboratory work and exposure age calculation

After crushing and sieving the samples to 200–700 μm, we applied standard lab procedures to obtain quartz and extract beryllium (Kohl and Nishiizumi 1992; Ochs and Ivy-Ochs 1997). The ^{10}Be/^{9}Be measurements for BS1, BS2 and GS1 were conducted with the TANDY Accelerator Mass Spectrometer (AMS) at the Laboratory of Ion Beam Physics, ETH Zurich. The measured ratios were normalized to the ETH Zurich in-house ^{10}Be/^{9}Be standard S2007 N with a nominal ratio of 28.10 ($\pm$ 0.76) $\times 10^{-12}$ (Christl et al. 2013). Our S2007N was calibrated relative to the ICN Be-10 AMS Std 01-5-1 with the revised ^{10}Be/^{9}Be ratio of 27.09 ($\pm$ 0.3) $\times 10^{-12}$ (See Table 2 in Nishiizumi et al. 2007) so it is tracable to NIST SRM. Two blanks were processed together with these samples. They had ^{10}Be/^{9}Be ratios of 0.003 ($\pm$ 0.001) $\times 10^{-12}$ and 0.014 ($\pm$ 0.002) $\times 10^{-12}$, i.e. at least ten times smaller than the sample ratios (Table 1). The blank ratios were subtracted from the sample ratios. Samples BS3–6 and GS2-5 were measured at DREAMS (DREsden AMS, Helmholtz-Zentrum Dresden-Rossendorf, 6MV) using the in-house standard SMD-Be-12 with a ^{10}Be/^{9}Be ratio of 1.704 ($\pm$ 0.030) $\times 10^{-12}$ (Akhmadaliev et al. 2013) traceable to the NIST-SRM 4325 standard with a ratio of 27.9 ($\pm$ 0.3) $\times 10^{-12}$ (Nishiizumi et al. 2007). One blank was processed together with the samples. It had ^{10}Be/^{9}Be ratios of 0.001 ($\pm$ 0.0003) $\times 10^{-12}$, i.e. mostly more than ten times smaller than the samples (Table 1). The blank ratios were again subtracted from the sample ratios before calculating the exposure ages.

We used the CRONUS Earth web calculator, v.2.0 (Marrero et al. 2016), the scaling system of Lifton et al. 2014), with a sea level high latitude production rate of 3.92 atoms/g/a (Borchers et al. 2016) and half-life time of of 1.387 Ma ($\pm$ 0.012), published by Korschinek et al. 2010) to calculate the ages. The same parameters are used when we recalculate published ages in the discussion section. Topographic shielding is < 1% for all samples and, thus, negligible, and no corrections were made for (negligible) effects related to snow and vegetation cover. All ages were calculated assuming zero erosion in order to yield minimum ages. In Table 1, we have also displayed the ages for an erosion rate $\varepsilon = 3$ mm/kyr because Ivy-Ochs et al. (2004) calculated this erosion rate on a granitic boulder $\sim$ 30 km northeast of Bern. Nevertheless, we only discuss the ages, calculated with zero erosion, as this is the minimum apparent age of the boulder. We used the same procedure for all recalculated ages from other publications.

Table 1 Sample data and surface exposure ages for the boulders dated in this study (BS1-6, GS1-5)

Name	Latitude (°N)	Longitude (°E)	Elevation (m asl)	Thickness (cm)	Quartz (g)	Carrier weight (mg)	[10]Be/[9]Be (10^{-12})	Conc. [10]Be (10^4 Atoms/g)	Production rate (Atoms g^{-1} a^{-1})	Age ε = 0 cm/ka (ka)	Age ε = 3 cm/ka (ka)
BS1	46.9144	7.4633	687	2	88.00	0.334	0.10 (± 0.007)	6.01 (± 0.45)	6.16	9.0 (± 1.0)	9 (± 1.0)
BS2	46.8859	7.4886	729	2	19.42	0.309	0.13 (± 0.009)	13.85 (± 1.03)	6.39	19.0 (± 2.0)	20.2 (± 2.2)
BS3	46.9424	7.5059	678	4	13.72	0.156	0.07 (± 0.003)	11.25 (± 0.52)	6.01	16.7 (± 1.5)	17.4 (± 1.6)
BS4	46.9397	7.5156	732	4	28.60	0.153	0.14 (± 0.004)	11.01 (± 0.34)	6.30	15.6 (± 1.3)	16.2 (± 1.4)
BS5	46.9393	7.5264	745	4	20.17	0.154	0.12 (± 0.003)	13.20 (± 0.37)	6.38	18.4 (± 1.5)	19.3 (± 1.6)
BS6	46.9400	7.5305	762	4	23.64	0.155	0.14 (± 0.004)	13.62 (± 0.35)	6.47	18.7 (± 1.4)	19.6 (± 1.6)
GS1	46.8664	7.4716	873	2	12.4	0.310	0.10 (± 0.008)	16.99 (± 1.39)	7.25	20.7 (± 2.2)	21.9 (± 2.5)
GS2	46.8527	7.4740	928	4	37.74	0.155	0.11 (± 0.003)	6.52 (± 0.19)	7.46	7.8 (± 0.6)	7.9 (± 0.6)
GS3	46.8515	7.4744	937	4	31.67	0.156	0.23 (± 0.011)	16.89 (± 0.77)	7.52	19.8 (± 1.7)	20.9 (± 1.9)
GS4	46.8512	7.4747	931	4	33.37	0.155	0.16 (± 0.004)	11.25 (± 0.29)	7.48	13.0 (± 1.0)	13.9 (± 1.1)
GS5	46.8494	7.4764	925	4	27.98	0.156	0.18 (± 0.005)	15.27 (± 0.38)	7.45	18.2 (± 1.5)	19.1 (± 1.6)

3 Results

All exposure ages are presented in Tab. 1 and illustrated in Fig. 3. The ages for Gurten Stade range from 7.8 ± 0.6 ka to 20.7 ± 2.2 ka and those for the Bern Stade range from 9.0 ± 1.0 ka to 19.0 ± 2.0 ka calculated without erosion. To find out, which ages are statistically the same, we use a χ^2 test with n − 1 degrees of freedom (n is the number of samples) published by Ward and Wilson (1978). This test has already been applied on [10]Be ages e.g. by Engel et al. (2017). The 95% critical values of the samples are calculated and compared with a theoretical value for χ^2. If the calculated χ^2 is bigger than the theoretical one, the age with biggest χ^2 is removed. This is repeated upon the calculated χ^2 is smaller than the theoretical value. Afterwards, the error weighted and arithmetic mean of each
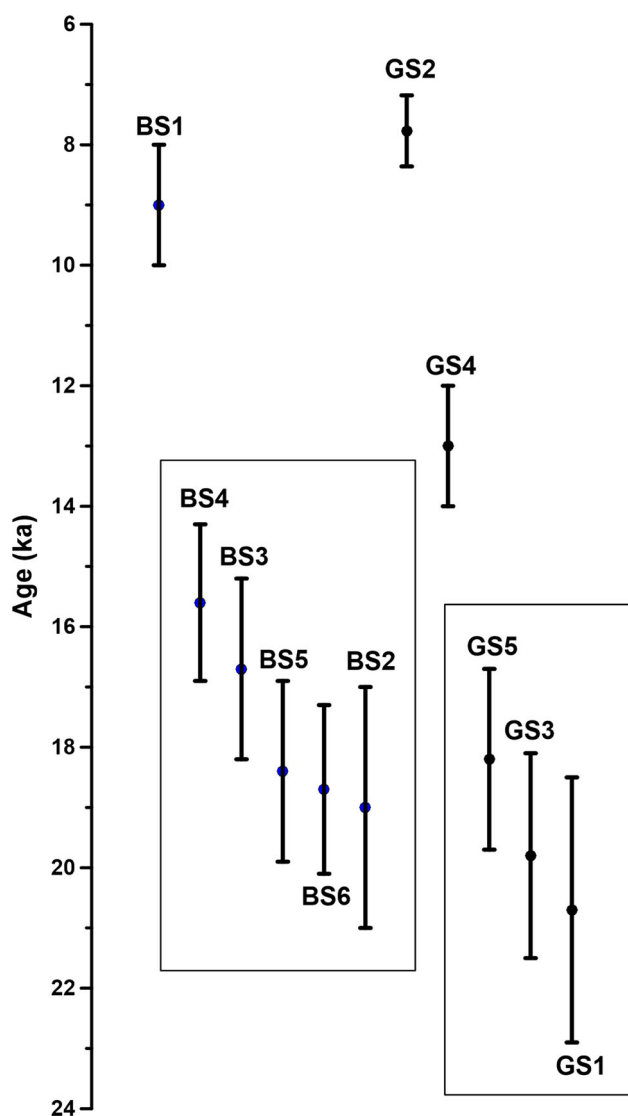
moraine was calculated. Gurten Stades yields an age of 19.27 (± 0.1) ka whereas GS 2 and GS 4 did not pass the test and are thus outliers. The average age for Bern Stade is 17.58 (± 0.61) ka. and BS 1 is an outlier. As both Stades have very similar ages, we also used this method for both Stades together: Using the Ward and Wilson (1978) approach for both moraines shows, that all samples but GS 2, GS 4 and BS 2 are statistically the same. The average age is 18.02 (± 0.56) ka.

4 Discussion

Although both moraines have statistically the same age, they are different from a stratigraphic point of view and were clearly deposited during different stades of the Aare glacier. That is why we use both stages in the discussion. As Heyman et al. (2011) suggests that the oldest ages are most reliable, we discuss the oldest ages which are accepted by the χ^2 test.

4.1 Regional context: glacial chronologies in northern Switzerland and the Alps

The ages reported in this study for the Bern and Gurten Stade (19.0 ± 2.0 ka and 20.7 ± 2.2 ka) fit very well into the regional glacial chronology for northern Switzerland (Fig. 3). Both ages are stratigraphically consistent with regard to recalculated surface exposure ages of ∼ 24 ka that have been reported for the local LGM of the merged Aare/Rhone Glacier (Ivy-Ochs et al. 2004). Moreover, the exposure ages are stratigraphically in good agreement with recently published exposure ages of which the oldest is 23 ± 2 ka from the LGM Reuss Glacier (re-calculated from Reber et al. 2014) and radiocarbon chronologies for the Linth and Rhine Glaciers (Fig. 3, Keller and Krayss 2005b).

The Gurten Stade likely documents a first major stillstand or re-advance of the Aare Glacier at 20.7 ± 2.2 ka. Compared to the Seftigschwand Stade, the ice thickness in the Aare Valley was already tens of meters less. The Gurten Stade probably correlates with a recessional stade of the Linth and Rhein Glacier, respectively, dated to ∼ 21 ka (Fig. 3; Keller and Krayss 2005a, b; Graf 2009; Preusser et al. 2011). Also an age from an Aare Glacier moraine (21.1 ± 1.8 ka), published by Akcar et al. (2011) has statistically the same age and might thus have been deposited by the receding LGM Aare Glacier in concert with the samples from Gurten Stade, presented in this study.

The Bern Stade then documents the last major re-advance of the Aare Glacier which ended at 19.0 ± 2.0 ka. Stratigraphically younger glacial deposits, referred to as

Fig. 3 All ages with total uncertainty. Data in the rectangle passed the χ^2 test

Muri, Wittigkofen and Schlosshalde Stades, respectively, have been mapped in and just south-east of Bern (Keller-hals et al. 2000), but only the Bern Stade has been explicitly described as re-advance. During the Bern Stade, the Aare and Rhone Glaciers must have been already separated. The exposure ages for the Bern Stade are in good agreement with an exposure age of 19.2 ± 1.7 ka of the moraine of the retreating Reuss Glacier (Reber et al. 2014). Moreover, correlations can be made to the Linth and Rhein Glaciers: The recessional moraines of the Rhein- and Linth glaciers (∼ 19 ka BP, Keller and Krayss 2005b) suggest a remarkable increase of the equilibrium line altitude after ∼ 18 ka and ice-free conditions in the Alpine forelands within 1–2 ka. This is consistent with the beginning of rapid ice surface lowering in the High Alps dated to ∼ 18.5 ka using cosmogenic nuclides (Wirsig et al. 2016).

The last glacial/deglacial chronology outlined above for northern Switzerland is consistent with chronostratigraphic results from other regions in the Alps. Starnberger et al. (2011), for example, described three stades for the Salzach Glacier in the eastern Alps of which the youngest two may correlate with Gurten and Bern Stade, based on available luminescence ages. Monegato et al. 2007) described three glacial stades for the Tagliamento Glacier in the Southern Alps, and available radiocarbon ages there suggest ice decay after ∼ 23, 21, and 19 ka, respectively. Several more recent studies corroborate a initial retreat right after the LGM during MIS 2 (> 23 ka) and final ice collapse after ∼ 18 ka in the southern Alps (Federici et al. 2012, 2016; Ravazzi et al. 2014; Scapozza et al. 2014; Gianotti et al. 2015).

5 Conclusions

In the present article, we have shown, that the first major still-stand/re-advance of the Aare Glacier (Gurten Stade) occurred at 20.7 ± 2.3 ka and that a second re-advance (Bern Stade) occurred at 19.0 ± 2.0 ka. Exposure dating in Switzerland is challenging, not only due to common post-depositional geomorphological processes, exposure ages can also be too young due to anthropogenic effects, i.e. quarrying, in the recent past. The now available chronology for the glaciation/deglaciation of the Aare/Rhone Glacier is in good agreement with published chronologies from northern Switzerland, from the Eastern and Southern Alps, as well as many glaciers and ice sheets worldwide.

References

Akçar, N., Ivy-Ochs, S., Kubik, P. W., & Schlüchter, C. (2011). Post-depositional impacts on 'Findlinge' (erratic boulders) and their implications for surface-exposure dating. *Swiss Journal of Geosciences, 104,* 445–453. https://doi.org/10.1007/s00015-011-0088-7.

Akhmadaliev, S., Heller, R., Hanf, D., Rugel, G., & Merchel, S. (2013). The new 6 MV AMS-facility DREAMS at Dresden. *Nuclear Instruments & Methods in Physics Research, Section B: Beam Interactions with Materials and Atoms, 294,* 5–10. https://doi.org/10.1016/j.nimb.2012.01.053.

Becker, P., Seguinot, J., Jouvet, G., & Funk, M. (2016). Last glacial maximum precipitation pattern in the Alps inferred from glacier modelling. *Geographica Helvetica, 71,* 173–187. https://doi.org/10.5194/gh-71-173-2016.

Bini, A., Buonchristiani, J.-F., Couterand, S., Ellwanger, D., Felber, M., Florineth, D., et al. (2009). *Die Schweiz während des letzteiszeitlichen Maximums (LGM)*. Wabern: Bundesamt für Landestopografie.

Borchers, B., Marrero, S., Balco, G., Caffee, M., Goehring, B., Lifton, N., et al. (2016). Geological calibration of spallation production rates in the CRONUS-Earth project. *Quaternary Geochronology, 31,* 188–198. https://doi.org/10.1016/j.quageo.2015.01.009.

Braucher, R., Brown, E. T., Bourlès, D. L., & Colin, F. (2003). In situ produced 10Be measurements at great depths: Implications for production rates by fast muons. *Earth and Planetary Science Letters, 211,* 251–258. https://doi.org/10.1016/S0012-821X(03)00205-X.

Christl, M., Vockenhuber, C., Kubik, P. W., Wacker, L., Lachner, J., Alfimov, V., et al. (2013). The ETH Zurich AMS facilities: Performance parameters and reference materials. *Nuclear Instruments & Methods in Physics Research, Section B: Beam Interactions with Materials and Atoms, 294,* 29–38. https://doi.org/10.1016/j.nimb.2012.03.004.

Dehnert, A., Preusser, F., Kramers, J. D., Akçar, N., Kubik, P. W., Reber, R., et al. (2010). A multi-dating approach applied to proglacial sediments attributed to the most extensive glaciation of the Swiss Alps. *Boreas, 39,* 620–632. https://doi.org/10.1111/j.1502-3885.2010.00146.x.

Engel, Z., Mentlík, P., Braucher, R., Křížek, M., Pluháčková, M., Arnold, M., et al. (2017). 10 Be exposure age chronology of the last glaciation of the Roháčská Valley in the Western Tatra Mountains, central Europe. *Geomorphology, 293,* 130–142. https://doi.org/10.1016/j.geomorph.2017.05.012.

Federici, P. R., Granger, D. E., Ribolini, A., Spagnolo, M., Pappalardo, M., & Cyr, A. J. (2012). Last glacial Maximum and the Gschnitz stadial in the Maritime Alps according to ^{10}Be cosmogenic dating. *Boreas, 41,* 277–291. https://doi.org/10.1111/j.1502-3885.2011.00233.x.

Federici, P. R., Ribolini, A., & Spagnolo, M. (2016). Glacial history of the Maritime Alps from the last glacial maximum to the little ice age. *Geological Society, London, Special Publications.* https://doi.org/10.1144/SP433.9.

Florineth, D., & Schlüchter, C. (2000). Alpine evidence for atmospheric circulation patterns in Europe during the last glacial maximum. *Quaternary Research, 54,* 295–308. https://doi.org/10.1006/qres.2000.2169.

Gianotti, F., Forno, M. G., Ivy-Ochs, S., Monegato, G., Pini, R., & Ravazzi, C. (2015). Stratigraphy of the Ivrea morainic

amphitheatre (NW Italy): an updated synthesis. *Alpine and Mediterranean Quaternary, 28*(1), 29–58.

Gosse, J. C., & Phillips, F. M. (2001). Terrestrial in situ cosmogenic nuclides: Theory and application. *Quaternary Science Reviews, 20,* 1475–1560. https://doi.org/10.1016/S0277-3791(00)00171-2.

Graf, H. R. (2009). *Stratigraphie von Mittel- und Spätpleistozän in der Nordschweiz*. Beiträge zur Geologischen Karte der Schweiz 168. Wabern: Bundesamt für Landestopografie swisstopo.

Graf, A., Akçar, N., Ivy-Ochs, S., Strasky, S., Kubik, P. W., Christl, M., et al. (2015). Multiple advances of Alpine glaciers into the Jura Mountains in the Northwestern Switzerland. *Swiss Journal of Geosciences, 108,* 225–238. https://doi.org/10.1007/s00015-015-0195-y.

Haeberli, W., Linsbauer, A., Cochachin, A., Salazar, C., & Fischer, U. H. (2016). On the morphological characteristics of overdeepenings in high-mountain glacier beds. *Earth Surface Processes and Landforms, 41,* 1980–1990. https://doi.org/10.1002/esp.3966.

Heinrich, H. (1988). Origin and consequences of cyclic ice rafting in the Northeast Atlantic Ocean during the past 130,000 years. *Quaternary Research, 29,* 142–152. https://doi.org/10.1016/0033-5894(88)90057-9.

Heisinger, B., Lal, D., Jull, A., Kubik, P., Ivy-Ochs, S., Knie, K., et al. (2002a). Production of selected cosmogenic radionuclides by muons: 2. Capture of negative muons. *Earth and Planetary Science Letters, 200,* 357–369. https://doi.org/10.1016/S0012-821X(02)00641-6.

Heisinger, B., Lal, D., Jull, A., Kubik, P., Ivy-Ochs, S., Neumaier, S., et al. (2002b). Production of selected cosmogenic radionuclides by muons: 1. Fast muons. *Earth and Planetary Science Letters, 200,* 345–355. https://doi.org/10.1016/S0012-821X(02)00640-4.

Hemming, S. R. (2004). Heinrich events: Massive late Pleistocene detritus layers of the North Atlantic and their global climate imprint. *Reviews of Geophysics*. https://doi.org/10.1029/2003RG000128.

Heyman, J., Stroeven, A. P., Harbor, J. M., & Caffee, M. W. (2011). Too young or too old: Evaluating cosmogenic exposure dating based on an analysis of compiled boulder exposure ages. *Earth and Planetary Science Letters, 302,* 71–80. https://doi.org/10.1016/j.epsl.2010.11.040.

Ivy-Ochs, S., Kerschner, H., Kubik, P. W., & Schlüchter, C. (2006a). Glacier response in the European Alps to Heinrich event 1 cooling: The Gschnitz stadial. *Journal of Quaternary Science, 21,* 115–130. https://doi.org/10.1002/jqs.955.

Ivy-Ochs, S., Kerschner, H., Reuther, A., Maisch, M., Sailer, R., Schaefer, J., et al. (2006b). The timing of glacier advances in the northern European Alps based on surface exposure dating with cosmogenic ^{10}Be, ^{26}Al, ^{36}Cl, and ^{21}Ne. *Geological Society of America Special Papers, 415,* 43–60. https://doi.org/10.1130/2006.2415(04).

Ivy-Ochs, S., Schäfer, J., Kubik, P. W., Synal, H.-A., & Schlüchter, C. (2004). Timing of deglaciation on the northern Alpine foreland (Switzerland). *Eclogae Geologicae Helvetiae, 97,* 47–55. https://doi.org/10.1007/s00015-004-1110-0.

Keller, O., & Krayss, E. (2005a). Der Rhein-Linth-Gletscher im letzten Hochglazial. 1. Teil: Einleitung; Aufbau und Abschmelzen des Rhein-Linth-Gletschers im oberen Würm. *Vierteljahrsschriften der Naturforschenden Gesellschaft Zürich, 150,* 19–32.

Keller, O., & Krayss, E. (2005b). Der Rhein-Linth-Gletscher im letzten Hochglazial. 2. Teil: Datierung und Modelle der Rhein-Linth-Gletscher. Klima Rekonstruktion. *Vierteljahrsschriften der Naturforschenden Gesellschaft Zürich, 150,* 69–85.

Keller, O., & Krayss, E. (2011). Mittel- und spätpleistozäne Stratigraphie und Morphogenese in Schlüsselregionen der Nordschweiz. *E&G – Quaternary Science Journal, 59,* 88–119. https://doi.org/10.3285/eg.59.1-2.08.

Kellerhals, P., Häfeli, C., & Staeger, D. (2000). *Geologischer Atlas der Schweiz: Blatt: 1166 Bern*. Wabern: Bundesamt für Landestopografie swisstopo.

Kohl, C., & Nishiizumi, K. (1992). Chemical isolation of quartz for measurement of in situ -produced cosmogenic nuclides. *Geochimica et Cosmochimica Acta, 56,* 3583–3587. https://doi.org/10.1016/0016-7037(92)90401-4.

Korschinek, G., Bergmaier, A., Faestermann, T., Gerstmann, U. C., Knie, K., Rugel, G., et al. (2010). A new value for the half-life of ^{10}Be by heavy-ion elastic recoil detection and liquid scintillation counting. *Nuclear Instruments & Methods in Physics Research, Section B: Beam Interactions with Materials and Atoms, 268,* 187–191. https://doi.org/10.1016/j.nimb.2009.09.020.

Lal, D. (1991). Lal, D. (1991). Cosmic ray labeling of erosion surfaces: In situ nuclide production rates and erosion models. *Earth and Planetary Science Letters, 104,* 424–439. https://doi.org/10.1016/0012-821X(91)90220-C.

Lifton, N., Sato, T., & Dunai, T. J. (2014). Scaling in situ cosmogenic nuclide production rates using analytical approximations to atmospheric cosmic-ray fluxes. *Earth and Planetary Science Letters, 386,* 149–160. https://doi.org/10.1016/j.epsl.2013.10.052.

Lisiecki, L. E., & Raymo, M. E. (2005). A Pliocene-Pleistocene stack of 57 globally distributed benthic δ 18 O records. *Paleoceanography*. https://doi.org/10.1029/2004PA001071.

Luetscher, M., Boch, R., Sodemann, H., Spötl, C., Cheng, H., Edwards, R. L., et al. (2015). North Atlantic storm track changes during the Last Glacial Maximum recorded by Alpine speleothems. *Nature Communications*. https://doi.org/10.1038/ncomms7344.

Marrero, S. M., Phillips, F. M., Borchers, B., Lifton, N., Aumer, R., & Balco, G. (2016). Cosmogenic nuclide systematics and the CRONUScalc program. *Quaternary Geochronology, 31,* 160–187. https://doi.org/10.1016/j.quageo.2015.09.005.

Monegato, G., Ravazzi, C., Donegana, M., Pini, R., Calderoni, G., & Wick, L. (2007). Evidence of a two-fold glacial advance during the last glacial maximum in the Tagliamento end moraine system (eastern Alps). *Quaternary Research, 68,* 284–302. https://doi.org/10.1016/j.yqres.2007.07.002.

Nishiizumi, K., Imamura, M., Caffee, M. W., Southon, J. R., Finkel, R. C., & McAninch, J. (2007). Absolute calibration of ^{10}Be AMS standards. *Nuclear Instruments & Methods in Physics Research, Section B: Beam Interactions with Materials and Atoms, 258,* 403–413. https://doi.org/10.1016/j.nimb.2007.01.297.

Ochs, M., & Ivy-Ochs, S. (1997). The chemical behavior of Be, Al, Fe, Ca and Mg during AMS target preparation from terrestrial silicates modeled with chemical speciation calculations. *Nuclear Instruments & Methods in Physics Research, Section B: Beam Interactions with Materials and Atoms, 123,* 235–240. https://doi.org/10.1016/S0168-583X(96)00680-5.

Phillips, F. M., Argento, D. C., Balco, G., Caffee, M. W., Clem, J., Dunai, T. J., et al. (2016). The CRONUS-earth project: A synthesis. *Quaternary Geochronology, 31,* 119–154. https://doi.org/10.1016/j.quageo.2015.09.006.

Preusser, F., & Graf, H. R. (2002). Erste Ergebnisse von Lumineszenzdatierungen eiszeitlicher Ablagerungen der Nordschweiz. *Jahresberichte und Mitteilungen des Oberrheinischen Geologischen Vereins, 84,* 419–438. https://doi.org/10.1127/jmogv/84/2002/419.

Preusser, F., Graf, H. R., Keller, O., Krayss, E., & Schlüchter, C. (2011). Quaternary glaciation history of northern Switzerland. *E&G Quaternary Science Journal, 60,* 282–305.

Preusser, F., Reitner, J. M., & Schlüchter, C. (2010). Distribution, geometry, age and origin of overdeepened valleys and basins in the Alps and their foreland. *Swiss Journal of Geosciences, 103,* 407–426. https://doi.org/10.1007/s00015-010-0044-y.

Preusser, F., & Schlüchter, C. (2004). Dates from an important early Late Pleistocene ice advance in the Aare valley, Switzerland. *Eclogae Geologicae Helvetiae, 97,* 245–253. https://doi.org/10.1007/s00015-004-1119-4.

Ravazzi, C., Pini, R., Badino, F., de Amicis, M., Londeix, L., & Reimer, P. J. (2014). The latest LGM culmination of the Garda Glacier (Italian Alps) and the onset of glacial termination. Age of glacial collapse and vegetation chronosequence. *Quaternary Science Reviews, 105,* 26–47. https://doi.org/10.1016/j.quascirev.2014.09.014.

Reber, R., Akçar, N., Ivy-Ochs, S., Tikhomirov, D., Burkhalter, R., Zahno, C., et al. (2014). Timing of retreat of the Reuss Glacier (Switzerland) at the end of the last glacial maximum. *Swiss Journal of Geosciences, 107,* 293–307. https://doi.org/10.1007/s00015-014-0169-5.

Reber, R., & Schlunegger, F. (2016). Unravelling the moisture sources of the Alpine glaciers using tunnel valleys as constraints. *Terra Nova, 28,* 202–211. https://doi.org/10.1111/ter.12211.

Scapozza, C., Castelletti, C., Soma, L., Dall'Agnolo, S., & Ambrosi, C. (2014). Timing of LGM and deglaciation in the Southern Swiss Alps. *Géomorphologie: Relief, Processus, Environnement, 20*(4), 307–322.

Schlüchter, C. (1976). *Geologische Untersuchungen im Quartär des Aaretals südlich von Bern: (Stratigraphie, Sedimentologie, Paläontologie)* (Beiträge zur geologischen Karte der Schweiz. Neue Folge). Bern: Stämpfli.

Schlüchter, C. (1987). Talgenese im Quartär: Eine Standortbestimmung. *Geographica Helvetica, 42,* 109–115. https://doi.org/10.5194/gh-42-109-1987.

Schlüchter, C. (1988). A non-classical summary of the Quaternary stratigraphy in the northern Alpine foreland of Switzerland. *Bulletin de la Société neuchâteloise de géographie, 23,* 143–157.

Ward, G. K., & Wilson, S. R. (1978). Procedures for comparing and combining radiocarbon age determinations: A critique: A CRITIQUE. *Archaeometry, 20,* 19–31. https://doi.org/10.1111/j.1475-4754.1978.tb00208.x.

Wirsig, C., Zasadni, J., Christl, M., Akçar, N., & Ivy-Ochs, S. (2016). Dating the onset of LGM ice surface lowering in the High Alps. *Quaternary Science Reviews, 143,* 37–50. https://doi.org/10.1016/j.quascirev.2016.05.001.